Thermal and Crystallization Behavior of Hydrogen-Bonded Miscible Blend of Poly(3-hydroxybutyrate) and Enzymatically Polymerized Polyphenol

Jianchun Li,[1] Tokuma Fukuoka,[2] Yong He,[1] Hiroshi Uyama,[3] Shiro Kobayashi,[2] Yoshio Inoue[1]

[1]*Department of Biomolecular Engineering, Tokyo Institute of Technology, Nagatsuta 4259-B-55, Midori-ku, Yokohama 226-8501, Japan*
[2]*Department of Materials Chemistry, Kyoto University, Nishikyo-ku, Kyoto 606-8510, Japan*
[3]*Department of Materials Chemistry, Osaka University, Yamadaoka 2-1, Suita, Osaka 565-0871, Japan*

Received 11 August 2003; accepted 30 December 2004
DOI 10.1002/app.22004
Published online in Wiley InterScience (www.interscience.wiley.com).

ABSTRACT: Enzymatically prepared novel polyphenol poly(4,4′-dihydroxydiphenyl ether) (PDHDPE) is blended to modify the properties of biodegradable polyester poly[(*R*)-3-hydroxybutyrate] (PHB). Because the differential scanning calorimetry data show a single composition-dependent glass transition for each blend, PHB and PDHDPE are found to be miscible in the amorphous phase. The crystallization of PHB is depressed by PDHDPE because PDHDPE reduces the molecular mobility and the flexibility of molecular chains of PHB. The Fourier transform IR spectra clearly indicate that PHB and PDHDPE interact through strong intermolecular hydrogen bonds between the carbonyl groups of PHB and the hydroxyl groups of PDHDPE. However, when PHB is blended with DHDPE monomer, no obvious hydrogen bonds are observed because of the phase separation and strong self-intermolecular hydrogen bonds between DHDPE molecules. © 2005 Wiley Periodicals, Inc. J Appl Polym Sci 97: 2439–2449, 2005

Key words: biodegradable; blends; miscibility; poly[(*R*)-3-hydroxybutyrate]; polyphenol

INTRODUCTION

It has been well recognized that using biodegradable polymers instead of traditional plastics is one of the ultimate available solutions to the environmental problems caused by the disposal of biostable plastic wastes. Isotactic poly[(*R*)-3-hydroxybutyrate] (PHB) is a polyester produced by microorganisms as carbon and energy reserves, and it has attracted much attention because of its biodegradability and biocompatibility.[1] Furthermore, the raw materials for the biosynthesis of PHB are renewable, which can avoid global warming induced by the use of nonrenewable sources like petroleum and coal. However, wider applications of PHB have been prevented because of its high manufacturing cost, low mechanical properties induced by high crystallinity and secondary crystallization, and narrow processing windows (i.e., its thermal degradation temperature is very close to its melting temperature).[1] Blending of PHB with a second component has been attempted.

In contrast, phenol–formaldehyde resins using novolaks and resols as prepolymers are widely used in industry because of their low manufacturing cost, dimensional stability, high tensile strength, and flame retardance.[2,3] However, an alternative process without formaldehyde for preparation of phenol polymers is strongly desired because of the toxic nature of formaldehyde. There has recently been an exponential increase of interest in the area of *in vitro* enzyme-catalyzed organic reactions. Enzymatic polymerization is defined as chemical polymer synthesis *in vitro* (in test tubes) via a nonbiosynthetic (nonmetabolic) pathway catalyzed by an isolated enzyme.[4] Enzymatic polymerization of phenols is thought to be an environmentally benign production process of formaldehyde-free polyphenols under mild reaction conditions. Furthermore, because the enzymatic process is based on analogies with biological heteropolymers like lignin and humic acid, it is reasonable to assume the biodegradability of enzymatically synthesized polyphenols. Actually, this assumption has been confirmed by the soil-system biodegradation of poly(*p*-ethyl phenol), poly(*m*-cresol), and poly(*p*-phenyl phenol).[5]

Enzyme horseradish peroxidase (HRP) has received considerable attention recently because of its availability, stability, and wide substrate range.[6] It has been reported that HRP is an effective catalyst for the oxidative polymerization of 4,4′-dihydroxydiphenyl ether (DHDPE).[7,8] Fourier transform IR (FTIR) and ^1H–^1H correlated NMR spectra show that the poly-

Correspondence to: Y. Inoue (yinoue@bio.titech.ac.jp).

(DHDPE) (PDHDPE) product is a mixture of phenylene and oxyphenylene units. It is believed that the phenolic hydroxyl groups in PDHDPE molecular chains have the ability to form intermolecular hydrogen bonds with the carbonyl groups of PHB. The introduction of intermolecular hydrogen bonds to polymer blends is an effective method to improve the miscibility between two components and modify the thermal and mechanical properties of the blend materials. Iriondo et al. reported that the crystallinity and melting temperature obviously decreased for PHB in hydrogen-bonded miscible blends with poly(*p*-vinyl phenol).[9,10] It is thought that the lower crystallinity and melting temperature would be beneficial to modify the mechanical properties and enlarge its processing windows.

In the present article, the miscibility and thermal properties of PHB/PDHDPE blends are investigated by differential scanning calorimetry (DSC). The spherulite growth rates of PHB in the blends are measured with polarized optical microscopy (POM). The intermolecular hydrogen-bonding interaction between PHB and PDHDPE is studied by FTIR spectroscopy. The spectra in the carbonyl region are analyzed with a curve-fitting program. Finally, the difference between the chemical structures of PDHDPE and DHDPE, which affect the formation of intermolecular hydrogen bonds, is discussed.

EXPERIMENTAL

Materials

Biosynthesized isotactic PHB [weight-average molecular weight (M_w) = 5.86 × 10^5, polydispersity (M_w/M_n) = 2.4] was supplied courtesy of Mitsubishi Gas Chemical Co., Inc. (Tokyo). PDHDPE [number-average molecular weight (M_n) = 1100, M_w/M_n = 1.1] was prepared by peroxidase-catalyzed oxidative polymerization of DHDPE using HRP as a catalyst in aqueous methanol.[7] The polymer precipitate was purified with aqueous methanol (50:50 vol %) in order to eliminate the low molecular weight monomer. PDHDPE consists of phenylene and oxyphenylene units with a low content of α,ω-hydroxyoligo(1,4-phenylene oxide)s.[8] Solvents (1,4-dioxane and chloroform) were purchased from Nacalai Tesque, Inc. (Kyoto, Japan) and Kanto Kagaku (Tokyo), respectively, and were used as received.

Preparation of blend samples

PHB/PDHDPE blend samples containing 0, 10, 20, 30, and 40 wt % PDHDPE were prepared by casting the mixed solution with an appropriate ratio of PHB in chloroform (2 wt %) and PDHDPE in 1,4-dioxane (2 wt %) on a Teflon petri dish as the casting surface. The films were placed under a vacuum for 1 week at room temperature to eliminate the solvent completely.

Thin layers of the PHB/PDHDPE blends with suitable thickness for FTIR measurements were prepared by casting the mixed solutions with appropriate ratios of PHB in chloroform and PDHDPE in 1,4-dioxane on the surface of silicon wafers (Mitsubishi Materials Corp., Tokyo). The silicon wafer used as a substrate is transparent for an IR incident beam. The maximum absorption of the resulting thin layer is about 1 AU, which ensures that the absorption is as high as possible and within the linear range of the detector at the same time. For this purpose, the concentration of PHB in the mixed solution was controlled at about 25 mg mL^{-1}. The samples were placed for 1 week under a vacuum to eliminate the solvent completely.

PHB/DHDPE blend samples were prepared by similar methods.

To indicate the blend composition, codes such as PHB/PDHDPE (90/10) and PHB/DHDPE (90/10) were used, where the numbers refer to the weight percentage of PHB and phenolic compounds (PDHDPE or DHDPE) in the blends, respectively. PHB, PDHDPE, and DHDPE are referred to as neat compounds.

Analytical procedures

DSC analysis

DSC thermograms were recorded on a Seiko DSC 220U (Seiko Instrument, Co., Tokyo) as follows: about 5 mg of PHB/PDHDPE blend sample was encapsulated into an aluminum pan and then heated from −50 to 200°C at a scanning rate of 20°C min^{-1} (first heating scan). The sample was rapidly quenched to −60°C and reheated from −50 to 200°C at a scanning rate of 20°C min^{-1} (second heating scan).

The melting temperature (T_m, first) was taken as the endothermic peak top in the thermal diagram recorded by the first heating scan, and the melting enthalpy (ΔH, first) was calculated from the integral of the endothermic melting peak in the DSC curve. The glass-transition temperature (T_g, second) was indicated by differentiation of the DSC peak recorded by the second heating scan.

Isothermal crystallization and measurement of the equilibrium melting temperature were carried out with a Pyris Diamond DSC (PerkinElmer Japan Co., Ltd., Yokohama, Japan). The instrument is routinely calibrated with high-purity indium and N_2 is used as a purge gas. All data acquisitions and analyses were performed using the Pyris software package. The crystallization and subsequent melting behavior of PHB/PDHDPE blends on the order of 7-mg mass were investigated from 100 to 112°C. Each sample was first melted at 200°C and held at this temperature for 2 min

to erase any prior thermal history. Then, the sample was quenched (about 80°C min^{-1}) to the crystallization temperature (T_c) and held at this temperature to crystallize. After isothermal crystallization was completed, the sample was heated to 200°C at a rate of 10°C min^{-1} to measure the T_m of the isothermally crystallized sample.

FTIR spectroscopy

FTIR measurements were carried out on a PerkinElmer Spectra 2000 FTIR spectrometer (PerkinElmer Japan Co., Ltd.) at room temperature under N_2 purging. All spectra were recorded at a resolution of 4 cm^{-1} with an accumulation of 64 scans.

Line-shape analysis of FTIR spectra

A curve-fitting program, based on the Gauss–Newton iteration procedure,[11] was applied for the line-shape analysis of the FTIR carbonyl vibration spectra. With the least-squares parameter adjustment criterion, the bands of carbonyl vibration can be quantitatively resolved into three parts: amorphous, crystalline, and hydrogen-bonded components. This fitting adjusts the peak position, line shape, peak width, and height in such a way that the best fit with an error of about 3% between experimental and calculated spectra was obtained.

POM

The measurement of spherulite growth rates was performed on an Olympus BX 90 polarizing microscope (Olympus Corp., Tokyo) equipped with a Fujix HC-2500 digital camera (Fuji Photo Film Co. Ltd., Tokyo). Polymer samples were placed between a microscope glass slide and a cover slip and heated with an FP82HT hot stage (Mettler Toledo International Inc., Tokyo). The samples (about 0.2 mg) were first heated to 190°C, kept for 3 min, and then cooled to the desired T_c with a cooling rate of 20°C min^{-1}. The spherulite growth rate was calculated as the slope of the line obtained by plotting the spherulite radius against the time.

RESULTS AND DISCUSSION

DSC analysis of phb/pdhdpe blends

It is well recognized that the observation of a single composition-dependent T_g between those of the neat polymer components can be taken as evidence of miscibility.[12,13] Because the glass transition of the polymer takes place in the amorphous phase for a semicrystalline polymer like PHB, the accurate value for the T_g can be obtained by the second scan of the DSC measurement as described in the Experimental section in order to eliminate or weaken the influence of the amorphous rigid interfacial region situated between the lamellar crystalline and amorphous phase.

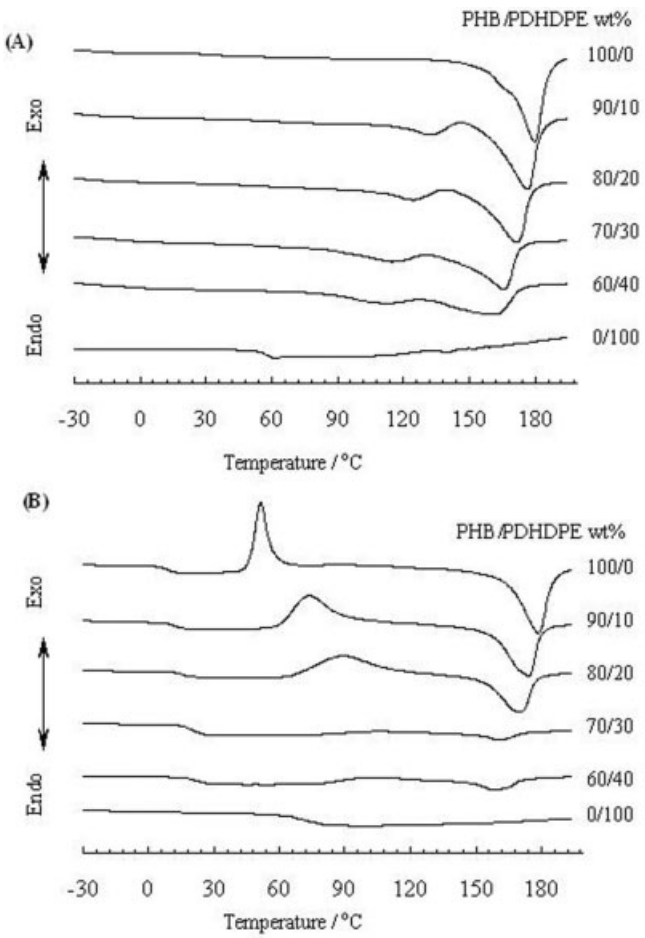

Figure 1 DSC traces of PHB/PDHDPE blends recorded during (A) the first and (B) the second heating scans at a scanning rate of 20°C min^{-1}.

Figure 1 shows the DSC traces of PHB/PDHDPE blends recorded during the first and second heating scans. The parameters of the thermal properties of PHB/PDHDPE blends are listed in Table I. The DSC traces of PHB show an endothermic peak at 179.5°C in the first scan and an increase of heat capacity at 9.5°C in the second scan, which are attributed to the melting of the crystalline domains and to the glass transition of the amorphous domains of PHB. The crystallinity of PHB in the blends (X^*) can be estimated from the ΔH in the first scan and the reference melting enthalpy of PHB with 100% crystallinity (ΔH_{ref}) via eq. (1):

$$X^* = \Delta H / (W_{PHB} \cdot \Delta H_{ref}) \quad (1)$$

where W_{PHB} is the weight fraction of PHB and ΔH_{ref} = 147 J g^{-1}.[14]

TABLE I
Thermal Properties and Crystallinity of PHB/PDHDPE Blends

Sample	T_{m1}[a] (°C)	ΔH (J g^{-1})	X*[b] (%)	T_{m2}[a] (°C)	T_g[c] (°C[c])	T_{cc}[c] (°C)
PHB	179.5	76 ± 8	52 ± 5	—	9.3	51.4
PHB/PDHDPE (90/10)	176.6	65 ± 7	49 ± 5	132.7	11.6	73.4
PHB/PDHDPE (80/20)	170.7	55 ± 5	47 ± 5	125.7	15.8	90.2
PHB/PDHDPE (70/30)	164.9	46 ± 5	44 ± 5	114.3	20.1	103.3
PHB/PDHDPE (60/40)	161.2	34 ± 3	38 ± 4	112.3	22.6	105.4
PDHDPE	—	—	—	—	66.1	—

[a] The T_m corresponding to the PHB component is obtained from the first DSC heating scan.
[b] Calculated from the melting enthalpy of the PHB component (the area of the DSC melting peak in the first heating scan) with the melting enthalpy of 100% crystalline PHB, assumed to be 147 J g^{-1}.
[c] Obtained from the second DSC heating scan.

As shown in Figure 1(A), two melting points are observed for all the blends. The T_m of neat PDHDPE is 120.2°C. With increasing the content of PDHDPE, the higher T_m (T_{m1}) corresponding to the PHB component decreases gradually from 179.5°C for neat PHB to 161.2°C in the PHB/PDHDPE (60/40) blend. A decrease of crystallinity for PHB is also observed from 51.6% for neat PHB to 38.3% for the PHB/PDHDPE (60/40) blend. Furthermore, this melting peak becomes broader with increasing content of PDHDPE. These phenomena suggest that the existence of PDHDPE influences the crystallization behavior of PHB because of the intermolecular interaction. The smaller and broader melting peak (corresponding to T_{m2}) prior to the major melting peak is also attributed to PHB. When the content of PDHDPE in the blends is less than 20%, the T_{m2} is higher than that of PDHDPE and decreases with increasing content of PDHDPE. When the content of PDHDPE is more than 20%, although the melting peak becomes too broad to get an accurate value of T_{m2}, it appears to be independent of the blend composition. Therefore, this melting peak is attributed to the melting of the eutectic mixture, which has been found in similar blend systems.[15]

It is not only the melting temperature and crystallinity of PHB that change, as shown in Figure 1(A), but also the T_g of PHB in the blends obviously shifts to a higher temperature, as shown in Figure 1(B). When increasing the content of PDHDPE in the blends, the T_g increased from 9.5 to 22.6°C. These changes of physical properties should be attributable to the existence of the interaction between PHB and PDHDPE. A probable interaction is the hydrogen-bonding interaction between the carbonyl groups in the PHB chains and the oxyphenylene units in the PDHDPE chains. Because of the formation of the intermolecular hydrogen bonds, PDHDPE might also act as a physical crosslinking agent in the blend, which would lower the flexibility of the PHB chain, resulting in the increase of the T_g.

In Figure 1(B), the DSC traces of PHB/PDHDPE blends show a cold crystallization peak of the PHB component after the glass transition. The area of the crystallization peak has a value similar to that of the melting peak, indicating that in the second heating scan the PHB component is almost in the amorphous state before the glass transition. The cold crystallization temperature (T_{cc}) of PHB increases from 51.6°C in the neat state to 105.4°C in the PHB/PDHDPE (60/40) blend. With the addition of PDHDPE to PHB, the blends show a higher glass transition, suggesting that the molecular motion of PHB is restrained. Because the crystallization of a polymer has a close relationship with the molecular motion of the polymer, the increase of T_{cc} confirms the existence of a strong intermolecular interaction between PHB and PDHDPE.

Crystallization kinetics of PHB/PDHDPE blends

The overall crystallization rate is determined by both the nucleation rate and the growth rate, and the nucleation process is the rate-controlled step. It is believed that, in the miscible PHB/PDHDPE blend system, the depression of crystallization of the crystallizable component (PHB) is attributed to numerous reasons such as the reduction of chain mobility and flexibility with the increase of the T_g, the dilution of PHB at the growth front, the change in free energy of nucleation as a result of specific interactions, and the competition between the advancing spherulite front and the diffusion of the noncrystallizable component into interlamellar and interfibrillar regions. The overall kinetics of isothermal crystallization is analyzed in terms of the Avrami equation[16–18]:

$$1 - X_c = \exp(-Kt_c^n) \tag{2}$$

where t_c is the time elapsed after the onset of crystallization; K is a temperature-dependent crystallization rate constant containing contributions from both the nucleation and growth rates; n is the so-called Avrami exponent, which depends on both the mode of nucleation and the dimensionality of the subsequent crystal

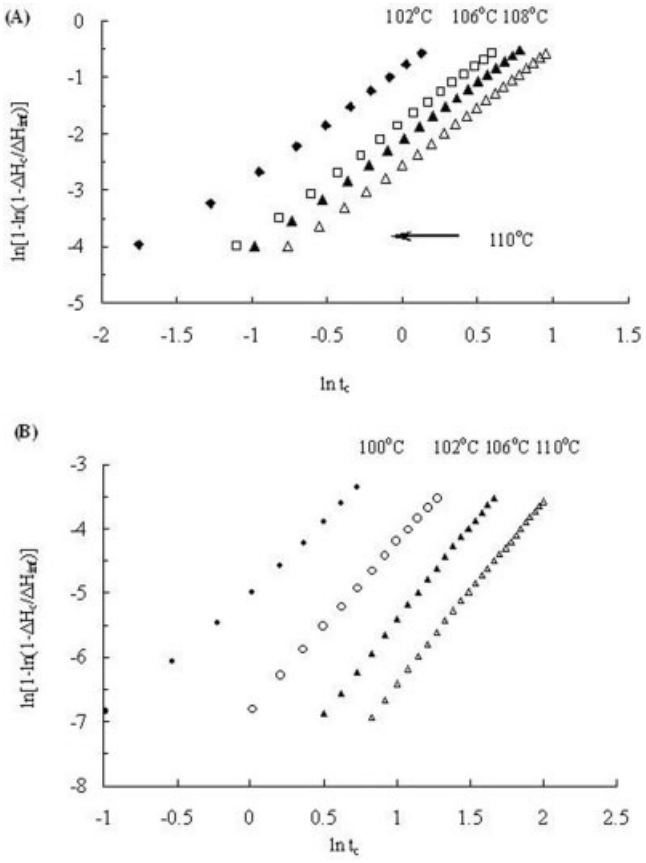

Figure 2 Typical linear Avrami plots showing the crystallization behavior of (A) PHB and (B) PHB/PDHDPE (80/20) blends.

growth; and X_c is the relative crystallinity, which can be calculated according to eq. (3):

$$X_c = \frac{\Delta H_c}{\Delta H_{\inf}} = \frac{\int_{t_0}^{t} (dH/dt)dt}{\int_{t_0}^{\infty} (dH/dt)dt} \quad (3)$$

where ΔH_c is the melting enthalpy of the sample at t_c and $\Delta H_{\inf}$ is the maximum melting enthalpy attained for the sample. Taking logarithms of eq. (3), eq. (4) is obtained.

$$\ln[-\ln(1 - X_c)] = \ln K + n \ln t_c \quad (4)$$

Plotting the left-hand side of the preceding against $\ln t_c$ should give a straight line of slope n and intercept $\ln K$. Figure 2 describes the typical linear Avrami plots of isothermal crystallization data obtained at various temperatures for PHB and the PHB/PDHDPE (80/20) blend. A very good linear relationship can be observed, which provides the calculation of the n and K values. The results for the PHB/PDHDPE blends studied here are listed in Table II. The values of n for PHB and all the blends are about 2.0 ± 0.3, suggesting that the addition of PHDPDE to PHB would not change the crystallization mechanism and the crystalline geometry of the PHB phase.

The crystallization half-time ($t_{1/2}$) is defined as the time required to reach $X_c = 0.5$. From n and K, it can be calculated according to eq. (5):

$$t_{1/2} = \left(\frac{\ln 2}{K}\right)^{1/n} \quad (5)$$

Figure 3 shows that the $t_{1/2}$ decreases for any composition when the T_c decreases because a larger supercooling would accelerate the crystallization process. Examining the dependence of the $t_{1/2}$ on the content of PDHDPE in the blends at the same T_c, the overall crystallization rate of PHB is depressed by the presence of PDHDPE. This could be explained by the fact that the molecular mobility and flexibility of PHB molecular chains are reduced by PDHDPE, as suggested by the increase of the T_g.

Equilibrium melting temperature of PHB/PDHDPE blends

Thermodynamic considerations predict that the chemical potential of a polymer will decrease with the addition of a second component as a miscible diluent. Furthermore, if the polymer is crystallizable, this decrease of chemical potential will result in the depres-

TABLE II
Avrami Parameters Obtained for PHB/PDHDPE Blends by Isothermal Crystallization

	PHB		PHB/PDHDPE (90/10)		PHB/PDHDPE (80/20)	
T_c (°C)	n	$K/(\min^{-n})$	n	K ($\min^{-n}$)	n	K ($\min^{-n}$)
100			1.7	9.2×10^{-2}	1.8	9.80×10^{-3}
102	1.9	4.35×10^{-1}	1.7	4.64×10^{-2}	1.9	4.30×10^{-3}
104	1.9	1.72×10^{-1}	2.0	1.80×10^{-2}	2.1	1.29×10^{-3}
106	2.0	1.58×10^{-1}	2.1	7.87×10^{-3}	2.2	7.33×10^{-4}
108	1.9	1.12×10^{-1}	2.2	6.41×10^{-3}	2.2	5.46×10^{-4}
110	2.0	8.60×10^{-2}	2.2	5.72×10^{-3}	2.3	1.94×10^{-4}
112	2.3	4.77×10^{-2}				

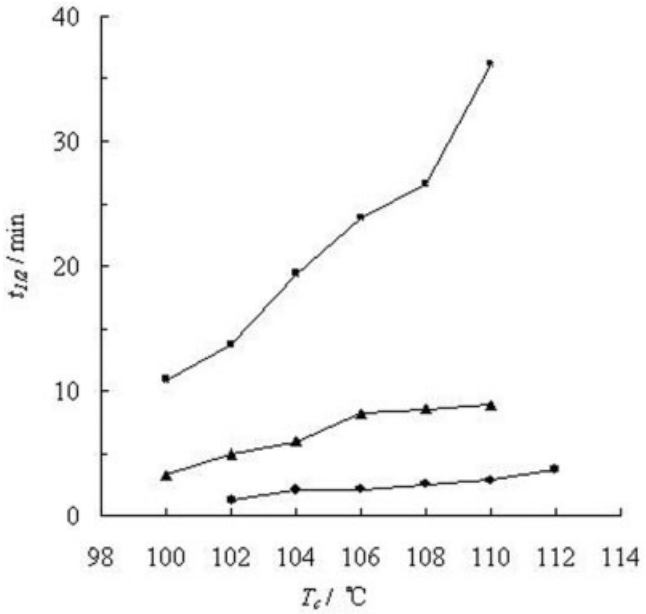

Figure 3 The crystallization half-time ($t_{1/2}$) as a function of T_c in PHB/PDHDPE blends: (●) PHB, (▲) PHB/PDHDPE (90/10), and (■) PHB/PDHDPE (80/20).

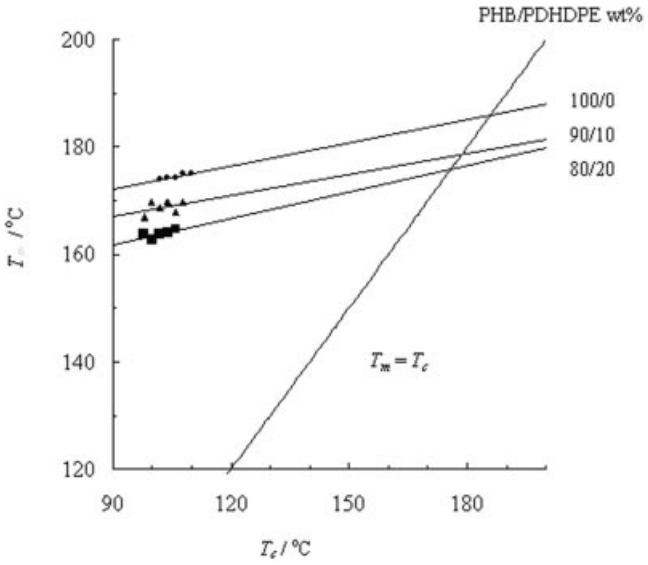

Figure 4 Hoffman–Weeks plots of PHB/PDHDPE blends: (●) PHB, (▲) PHB/PDHDPE (90/10), and (■) PHB/PDHDPE (80/20).

sion of the equilibrium melting temperature (T_m^0). The T_m^0, which may be defined as the melting point of infinitely large lamella, can be derived by the following Hoffman–Weeks equation:[19]

$$T_m = T_m^0(1 - 1/\gamma) + T_c/\gamma \quad (6)$$

where T_m is the observed melting temperature, T_c is the isothermal crystallization temperature, and γ is the ratio of the initial to the final lamellar thickness. The Hoffman–Weeks equation indicates a linear relation between T_m and T_c. Therefore, extrapolating to $T_m = T_c$ would give the T_m^0 of a perfect polymer crystal with infinite lamella thickness.

Figure 4 presents the Hoffman–Weeks plots for PHB and its blends with PDHDPE. A linear dependence of the T_m on the T_c is observed for all cases. The T_m^0 can be obtained by plotting the T_m as a function of the blend composition with a linear least-squares fit via an extrapolation of the linear data until intersection with the $T_m = T_c$ line. Figure 5 plots the T_m^0 as a function of the blend composition. The T_m^0 of neat PHB is determined to be 186.0°C, the value of which is slightly higher than that reported in the literature because of the higher molecular weight sample used here.[20] With increasing content of PDHDPE in the blends, the depression of T_m^0 for the PHB fraction in these blends is observed. When the content of PDHDPE reaches 20%, the T_m^0 decreases to 176.0°C. The depression of the T_m^0 provides additional evidence for the miscibility between PHB and PDHDPE

Spherulite growth rates of PHB

It is well known that the crystallization of polymers with sufficient structural regularity can occur over a range of temperatures limited by the T_g and the T_m^0. When the desired T_c locates toward the T_g, the crystallization kinetics would be controlled by the chain mobility, such that the rate increases with increasing T_c (viscosity decreasing) in this mobility regime, whereas the crystallization rate would be governed by the thermodynamic driving force of crystallization (the thermodynamically controlled regime) if the de-

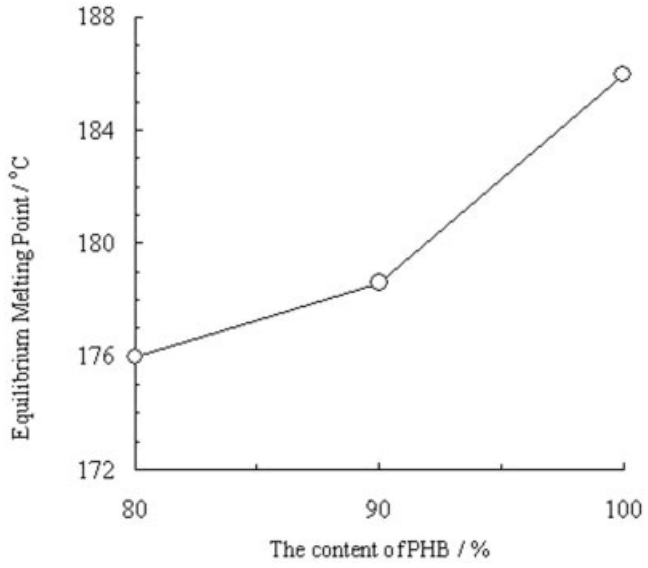

Figure 5 The equilibrium melting point depression of PHB/PDHDPE blends.

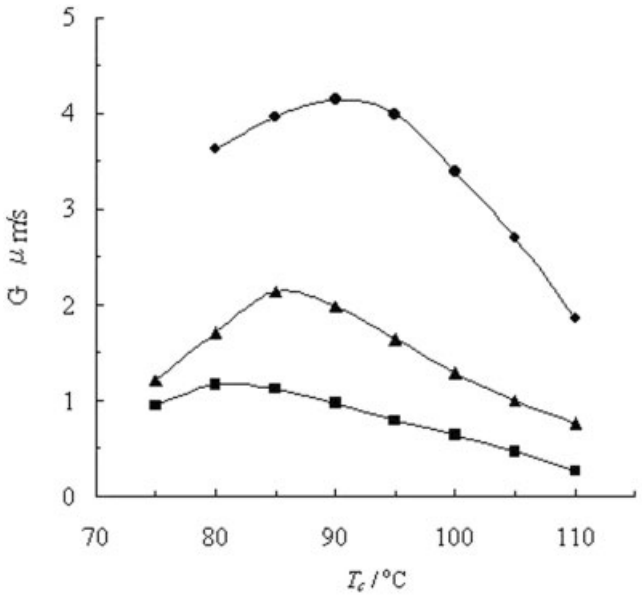

Figure 6 The PHB spherulite growth rate of PHB/PDHDPE blends: (●) PHB, (▲) PHB/PDHDPE (90/10), and (■) PHB/PDHDPE (80/20).

sired T_c locates toward the T_m^0.[21] The interplay between these two factors produces a maximum in the crystallization rate at T_m^{max} between the T_g and T_m^0. The effect of PDHDPE on the spherulite growth rates of PHB in the neat state and in the blends would be determined by observation with a POM microscope in the range from 75 to 110°C. The spherulite growth rate is constant until impingement takes place. Figure 6 depicts the variation of the PHB spherulite growth rate (G) with the content of PDHDPE at various T_c values. The T_m^{max} values for PHB and its blend with different PDHDPE contents are observed. With increasing content of PDHDPE in the blends, the T_m^{max} shifts to a lower temperature and the rate of spherulite growth at a given T_c decreases. It is thought that the existence of amorphous PDHDPE as a dilution effect would result in the diminution of the formation of a critical nucleus on the front of the growing spherulite. Furthermore, the decreasing segmental mobility of PHB molecules and the decrease in undercooling due to the T_m^0 depression are not favorable for the spherulite growth of PHB in the blends.

FTIR analysis of PHB/PDHDPE blends

FTIR spectroscopy is a quite suitable technique to investigate specific intermolecular interactions. The changes of the strength and position of IR absorption peaks resulting from some characteristic functional groups can be attributed to the existence of intermolecular or intramolecular interaction.

As a proton donor, PDHDPE has excellent potential to form hydrogen bonds because of its phenolic hydroxyl groups. It is well known that, for the PHB/PDHDPE blends studied here, the carbonyl groups of PHB yield a $\nu_{C=O}$ stretching mode at 1725 cm^{-1}, but PDHDPE has no group that produces absorption in the region from 1650 to 1800 cm^{-1}. Therefore, it is taken for granted that any changes in the FTIR spectra in this region should be directly attributed to the change of the chemical environment of carbonyl groups, such as the formation of hydrogen bonds. Figure 7(A) shows the FTIR spectra of PHB/PDHDPE blends in the carbonyl vibration region as a function of PDHDPE composition. When PHB is blended with PDHDPE, the spectra show obvious changes when increasing the content of PDHDPE. The spectra become broader and in the high wavenumber show strong absorption at 1741 cm^{-1}, suggesting that the content of molecular chains in the amorphous phase increases. Furthermore, in addition to the band centered at 1725 cm^{-1}, an absorption band centered at 1709 cm^{-1} increases in the lower wavenumber, the phenomenon of which is the so-called redshift as a characteristic of the vibration of the hydrogen-bonded carbonyl groups. The explanation is that the existence of the electronegative oxygen atom causes the carbonyl group to be highly polarized, the carbon atom

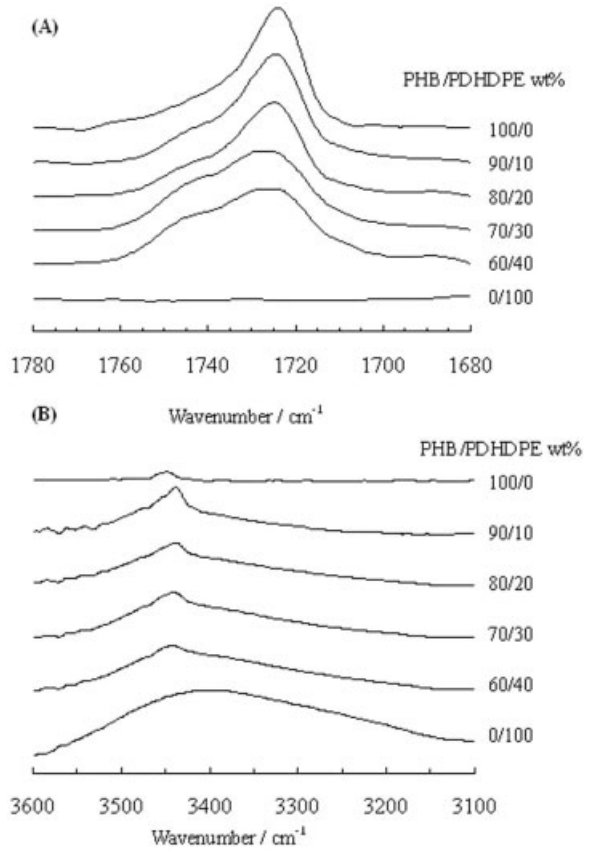

Figure 7 FTIR spectra of PHB/PDHDPE blends in the vibration region of (A) carbonyl groups and (B) hydroxyl groups.

bears a substantial positive charge, and the oxygen atom bears a substantial negative charge. At the same time, the benzene ring of phenol acts as an electron-withdrawing group to hold the proton of a hydroxyl group less strongly. All of these lead to the formation of intermolecular hydrogen bonds between the carbonyl groups of PHB and the hydroxyl groups of PDHDPE. We observed that the relative absorbance of this hydrogen-bonded carbonyl vibration increased with the content of PDHDPE in the blends. However, at the same time, the relative vibration absorbance of the free carbonyl groups (not hydrogen-bonded carbonyl groups in the amorphous and crystalline phase) was reduced, which suggests more PHB molecules involved in hydrogen bonds.

Figure 7(B) provides the FTIR spectra of PHB/PDHDPE blends in the hydroxyl vibration region as a function of the PDHDPE composition. A very weak absorption peak centered at 3456 cm^{-1} is attributed to the vibration of hydroxyl groups at the chain terminal of PHB. In the spectrum for neat PDHDPE, there is a wide band centered at 3400 cm^{-1}, which should be mainly assigned to the free and self-hydrogen-bonded hydroxyl groups in neat PDHDPE because of its relatively low wavenumber. When PHB is blended with PDHDPD, we found that the vibration of hydroxyl groups is located between 3400 and 3456 cm^{-1} and the absorption peak shifts to a higher wavenumber with increasing content of PDHDPE. This confirms the formation of intermolecular hydrogen bonds between the carbonyl groups of PHB and the hydroxyl groups of PDHDPE. Furthermore, we concluded that PDHDPE is inclined to form self-intermolecular hydrogen bonds (PDHDPE—OH· · ·OH—PDHDPE) rather than intermolecular hydrogen bonds (PDHDPE—OH· · · O═PHB), as revealed by the comparison of two types of hydrogen bonds.

Quantitative analysis of fractions of hydrogen-bonded carbonyl groups

As discussed above, the FTIR spectra confirmed qualitatively that intermolecular hydrogen bonds were formed between the carbonyl groups of PHB and the hydroxyl groups of PDHDPE. Here, a curve-fitting program based on the Beer–Lambert law is used for quantitative analysis of the formation of the intermolecular hydrogen bond.[22]

The spectra of PHB/PDHDPE blends in the carbonyl region exhibit three distinct components. The components at approximately 1741 and 1725 cm^{-1} could be attributed to PHB in the amorphous and crystalline conformations, respectively, and the component observed at 1709 cm^{-1} could be attributed to the hydrogen-bonded carbonyl vibration as previously discussed. A curve-fitting program is employed to quantitatively analyze the spectra regarding the integrated intensity of these three separated bands. As an example, Figure 8 illustrates the experimental and fitted spectra for the PHB/PDHDPE (70/30) blend in the carbonyl vibration region. The experimental spectrum is divided into three peaks for the amorphous, crystalline, and hydrogen-bonded components. It is very easy to attain their data of integrated intensity. The excellent agreement between the experimental and fitted spectra indicates the reliability of this fitting technique. The fraction of the carbonyl groups involved in the intermolecular hydrogen bond [$F_{(B,CO)}$] could be calculated according to eq. (7)[10,23]:

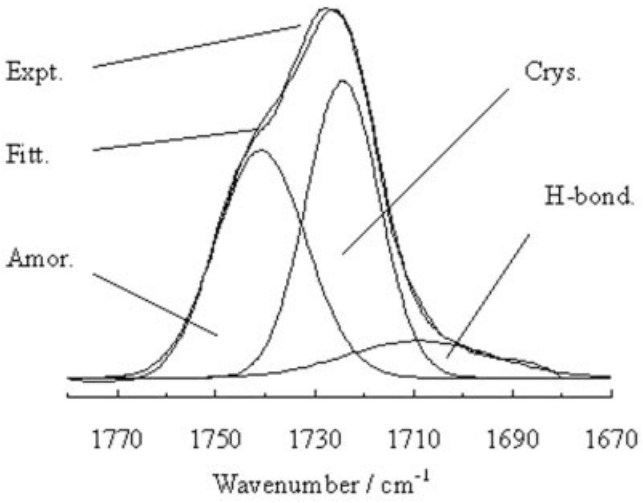

Figure 8 Experimental and fitted spectra of the PHB/PDHDPE (70/30) blend in the carbonyl vibration region. Expt., the experimental spectrum; Amor., the amorphous component; Crys., the crystalline component; H-bond., the hydrogen-bonded component; Fitt, the fitted spectrum, that is, the sum of the amorphous, crystalline, and hydrogen-bonded components.

$$F_{(B,CO)} = A_{(B,CO)}/(A_{(B,CO)} + A_{(A,CO)} \cdot \gamma_{B/A} + A_{(C,CO)} \cdot \gamma_{B/C}) \quad (7)$$

where $A_{(B,CO)}$, $A_{(A,CO)}$, and $A_{(C,CO)}$ are the integrated intensities corresponding to the hydrogen-bonded, amorphous, and crystalline carbonyl bands, respectively; and $\gamma_{B/A}$ and $\gamma_{B/C}$ are the absorption ratios when the difference between the absorbances of the hydrogen-bonded and the amorphous carbonyl groups and between those of the hydrogen-bonded and the crystalline carbonyl groups, respectively, are considered, because it has been shown that the absorption coefficient is a function of the frequency shift.[24] They are defined as

$$\gamma_{i/j} = \int_0^{+\infty} \varepsilon_i(\nu) d\nu / \int_0^{+\infty} \varepsilon_j(\nu) d\nu \quad (8)$$

TABLE III
Relative Intensities and Fractions of Hydrogen-Bonded Carbonyl Groups for PHB/PDHDPE Blends

Sample	$A_{(CO)}/\Sigma A \times 100$ (%)	$A_{(C,CO)}/\Sigma A \times 100$ (%)	$A_{(B,CO)}/\Sigma A \times 100$ (%)	$F_{(B,CO)}$
PHB	31 ± 1	69 ± 2	0	0
PHB/PDHDPE (90/10)	30 ± 1	62 ± 2	8 ± 1	0.055
PHB/PDHDPE (80/20)	34 ± 1	56 ± 2	11 ± 1	0.073
PHB/PDHDPE (70/30)	43 ± 1	46 ± 1	11 ± 1	0.078
PHB/PDHDPE (60/40)	44 ± 1	38 ± 1	18 ± 1	0.125

where $\varepsilon_i(\nu)$ and $\varepsilon_j(\nu)$ are the absorbances of i and j components; ν is the wavenumber; and i and j are A, B, or C. The values of $\gamma_{B/A}$ and $\gamma_{B/C}$ were measured and found to be 1.5.[15]

Based on the theoretical analysis, Table III provides the data of the fractions of the hydrogen-bonded carbonyl groups for the blends of PHB and PDHPDE. It is obvious that $A_{(C,CO)}$ has the tendency to decrease with increasing content of PDHDPE, which is identical to the results of DSC. Furthermore, at the same time, the values of $A_{(B,CO)}$ and $F_{(B,CO)}$ are notably increased with increasing content of PDHDPE. The value of $F_{(B,CO)}$ is less than 0.13 in PHB/PDHDPE (60/40). However, in another similar blend system of poly(ε-caprolactone) (PCL)/PDHDPE, the value is 0.18.[25] It is believed that the methyl groups in PHB chains hinder the formation of hydrogen bonds with PDHDPE.

Properties of PHB/DHDPE blends

We reported that the monomer bisphenol DHDPE has the ability to form intermolecular hydroxyl bonds with a biodegradable polyester PCL.[26] The existence of intermolecular hydrogen bonds between the hydroxyl groups of DHDPE and the carbonyl groups of PHB is taken for granted. However, it is not the case. Figure 9 presents the FTIR spectra of PHB/DHDPE blends. The hydrogen-bonding characteristic peak in the vibration of the PHB carbonyl groups is not observed. It can be explained by two reasons: the self-intermolecular hydrogen-bonding interaction between DHDPE molecules is so strong that it is very difficult for PHB to form intermolecular hydrogen bonds with DHDPE; in the preparation of samples, phase separation takes place with the evaporation of

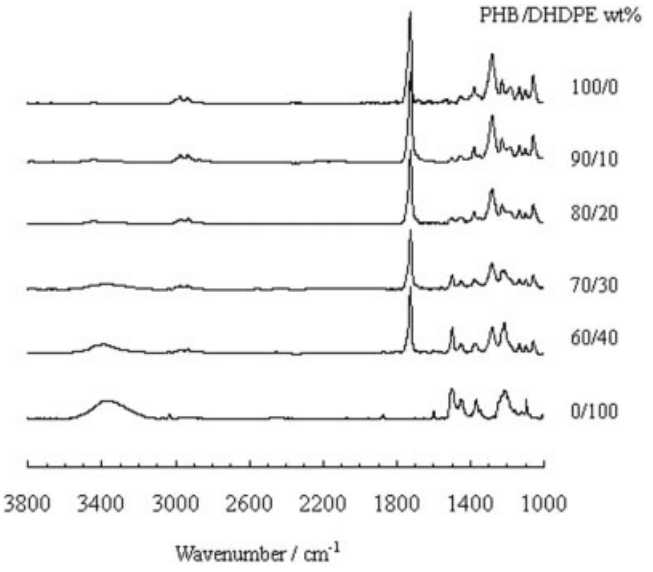

Figure 9 FTIR spectra of PHB/DHDPE blends in the 1000–3800 cm^{-1} region.

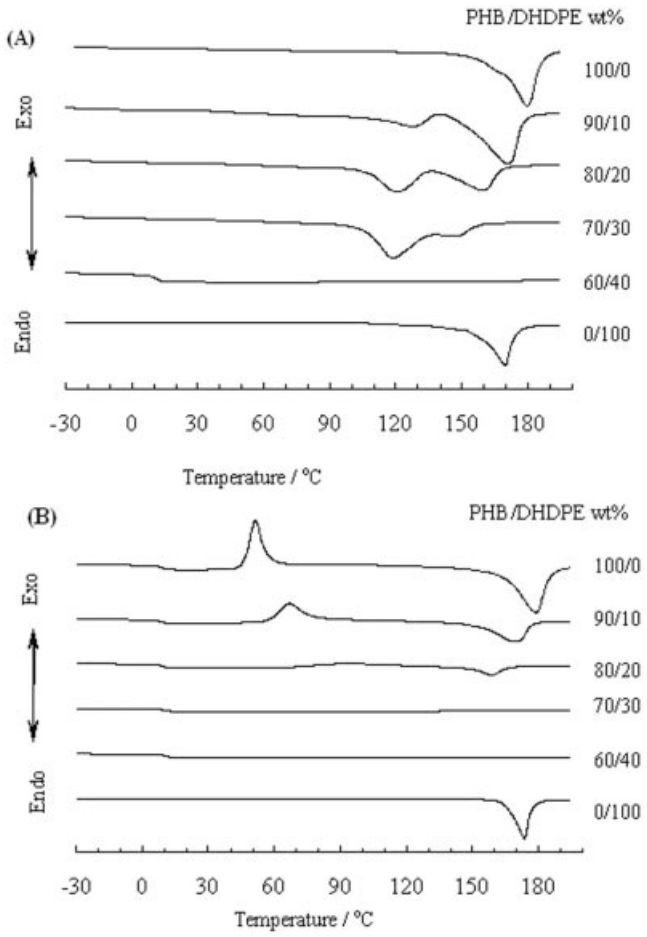

Figure 10 DSC traces of PHB/DHDPE blends recorded during (A) the first and (B) the second heating scans at a scanning rate of 20°C min^{-1}.

TABLE IV
Thermal Properties and Crystallinity of PHB/DHDPE Blends

Sample	T_{m1}[a] (°C)	ΔH (J g^{-1})	X*[b] (%)	T_{m2}[a] (°C)	T_g[c] (°C[c])	T_{cc}[c] (°C)
PHB	179.5	76 ± 8	52 ± 5	—	9.3	51.4
PHB/DHDPE (90/10)	170.2	63 ± 6	47 ± 5	127.3	8.4	67.4
PHB/DHDPE (80/20)	159.1	28 ± 3	24 ± 2	121.0	9.1	94.2
PHB/DHDPE (70/30)	145.5	5.4 ± 1	5.3 ± 1	118.0	11.1	—
PHB/DHDPE (60/40)	130.2	—	—	118.6	11.1	—
DHDPE	171.7	126 ± 13	—	—	—	—

[a] The T_m corresponding to the PHB component is obtained from the first DSC heating scan.
[b] Calculated from the melting enthalpy of the PHB component (the area of the DSC melting peak in the first heating scan) with the melting enthalpy of 100% crystalline PHB, assumed to be 147 J g^{-1}.
[c] Obtained from the second DSC heating scan.

solvent. However, the addition of DHDPE would modify the thermal properties of PHB.

Figure 10 provides the DSC traces of PHB/DHDPE blends recorded in the first and second scans. The parameters of the thermal properties of PHB/DHDPE blends are listed in Table IV. In Figure 10(A), when PHB is blended with DHDPE, PHB shows two melting peaks. When the content of DHDPE increases in the blends, the higher one (T_{m1}) shifts to a lower temperature and the lower one (T_{m2}) stays almost constant. In the PHB/DHDPE (60/40) blend, the PHB becomes completely amorphous. It is suggested that, with the addition of DHDPE to PHB, the crystallization of PHB is depressed and eutectic mixtures are formed. In Figure 10(B), the DSC traces of PHB/DHDPE blends in the second heating scan show similar thermal phenomena observed for PHB/PDHDPE blend systems, such as the cold-crystallization peak of PHB and the single glass transition. Furthermore, the crystallization of PHB is obviously depressed because the cold-crystallization enthalpy and melting enthalpy decrease, in addition to the fact that the blends cannot crystallize when the content of DHDPE is more than 30%. We believe that the existence of DHDPE impedes the formation of a critical nucleus for PHB.

It is interesting to point out that all blends show one glass transition at the temperature very close to that of neat PHB. In polymer blend systems, this phenomenon usually indicates that there is very weak or even no intermolecular hydrogen-bonding interaction between two components. This seems consistent with the FTIR results. However, for the blend system involving the low molecular weight phenol compound DHDPE, it is not the case. In the FTIR measurement, the intermolecular hydrogen-bonding interaction between PHB and DHDPE cannot be observed because of the phase separation and the strong self-intermolecular hydrogen-bonding interaction between DHDPE molecules.

In order to crosslink PHB, one phenolic hydroxyl group of one DHDPE molecule should form an intermolecular hydrogen bond with one PHB molecule and the other hydroxyl group should also form another intermolecular or self-intermolecular hydrogen bond; that is, one DHDPE molecule has to form two hydrogen bonds at the same time. The existence of side chains (methyl groups) on PHB molecules makes it difficult for PHB to be crosslinked by DHDPE and the T_g of the blends stays almost constant. Obviously, polyesters without side chains like PCL are easier to crosslink with the addition of DHDPE by intermolecular hydrogen-bonding interactions.[26]

CONCLUSION

A systematic study of the thermal and crystallization behavior of PHB/PDHDPE blends was performed. We found that the blends were miscible and the crystallization behavior of PHB was strongly influenced by the blend composition and crystallization temperature. With the addition of PDHDPE, the melting temperature of PHB was depressed. We concluded that the introduction of intermolecular hydrogen bonds is an effective method to enlarge the processing window of PHB. The phase separation phenomenon in PHB/DHDPE suggested that phenol groups in the enzymatically polymerized PDHDPE have a higher tendency to form hydrogen bonds to modify the properties of polyesters than those in the monomer DHDPE.

References

1. Doi, Y. Microbial Polyesters; VCH: New York, 1990.
2. Ma, C. C. M.; Wu, H. D.; Lee, C. T. J Polym Sci Part B: Polym Phys 1998, 36, 1721.
3. Huang, M. W.; Kuo, S. W.; Wu, H. D.; Chang, F. C.; Fang, S. Y. Polymer 2002, 43, 2479.
4. Kobayashi, S.; Uyama, H.; Kimura, S. Chem Rev 2001, 101, 3793.
5. Farrell, R.; Ayyagari, M.; Akkara, J.; Kaplan, D. J Environ Polym Degrad 1998, 6, 115.
6. Marx, K. A.; Zhou, T.; Sarma, R. Biotechnol Prog 1999, 15, 522.
7. Uyama, H.; Maruichi, N.; Tonami, H.; Kobayashi, S. Biomacromolecules 2002, 3, 187.
8. Fukuoka, T.; Tonami, H.; Maruichi, N.; Uyama, H.; Kobayashi, S. Macromolecules 2000, 33, 9152.

9. Iriondo, P.; Iruin J. J.; Fernandez-Berride, M. Polymer 2000, 36, 3235.
10. Iriondo, P.; Iruin J. J.; Fernandez-Berride, M. Macromolecules 1996, 29, 5605.
11. He, Y.; Inoue, Y. Polym Int 2000, 49, 623.
12. Aubin, M.; Prud'homme, R. E. Macromolecules 1988, 21, 10.
13. Bisso, G.; Casarino, P.; Pedemonte, E. Thermochim Acta 1998, 321, 81.
14. Barham, P. J.; Keller, A.; Otun, E. L.; Holmes, P. A. J Mater Sci 1984, 19, 2781.
15. He, Y.; Asakawa, N.; Inoue, Y. J Polym Sci Part B: Polym Phys 2000, 38, 2891.
16. Avrami, M. J Chem Phys 1939, 7, 1103.
17. Avrami, M. J Chem Phys 1940, 8, 212.
18. Avrami, M. J Chem Phys 1941, 9, 177.
19. Hoffman, J. D.; Weeks, J. J. J Chem Phys 1965, 42, 4301.
20. Yam, W. Y.; Ismail, J.; Kammer, H. W.; Schmidt, H.; Kummerlöwe, C. Polymer 1999, 40, 5545.
21. You, J. W.; Chiu, H. J.; Don, T. M. Polymer 2003, 44, 4355.
22. Sanchis, A.; Prolongo, M. G.; Salom, C.; Masegossa, M. R. J Polym Sci Part B: Polym Phys 1998, 36, 95.
23. Li, D.; Brisson, J. Polymer 1998, 39, 793.
24. Skrovanek, D. J.; Howe, S. E.; Painter, P. C.; Coleman, M. M. Macromolecules 1988, 21, 346.
25. Li, J.; Fukuoka, T.; He, Y.; Uyama, H.; Kobayashi, S.; Inoue, Y. J Polym Sci, submitted.
26. Li, J.; He, Y.; Inoue, Y. J Polym Sci Part B: Polym Phys 2001, 39, 2108.